MODELING DISTRIBUTED HYDROLOGICAL AND SEDIMENT PROCESSES TO ASSESS LAND USE EFFECTS IN CHAO PHRAYA RIVER BASIN

Kazuki Tanuma[1], Zuliziana Suif [2], Atchara Komsai[3], Winai Liengcharernsit[4] , and Oliver Cristian Saavedra Valeriano[5]

[1] Department of Civil Engineering, Tokyo Institute of Technology,
Tokyo, Japan, e-mail: tanuma.k.aa@m.titech.ac.jp
[2] Department of Civil Engineering, Tokyo Institute of Technology,
Tokyo, Japan, e-mail: suif.z.aa@m.titech.ac.jp
[3] Interdisciplinary Graduate School of Science and Engineering, Tokyo Institute of
Technology,Yokohama, Japan, e-mail: komsai.a.aa@m.titech.ac.jp
[4] Faculty of Engineering, Kasetsart University,Bangkok, Thailand, e-mail: fengwnl@ku.ac.th
[5] Department of Civil Engineering, Tokyo Institute of Technology, Tokyo, Japan,
e-mail: saavedra.o.aa@m.titech.ac.jp

Abstract

Soil loss and its transport processes were coupled with an existing distributed hydrological model to assess the effects of land use change on stream flow and suspended sediment load in the Chao Phraya River basin, Thailand. The simulation period spanned from 2001 to 2010. The results indicate that the Nash–Sutcliffe efficiency of upper sub-basins fluctuated in the range 0.51–0.72, indicating the applicability of the model for long-term simulation at the monthly scale. Land use change during 2001–2010 caused a 1.6% increase in suspended sediment load based on the present trend. The changes were particularly pronounced in the Wang River basin, where the delivery ratio was highest. Moreover, the urbanization and conversion of farm land from paddy fields exerted negative effects on sediment runoff in Chao Phraya River basin. The proposed model has the ability to quantitatively evaluate the heterogeneity of sediment runoff in the basin, demonstrating the benefits and trade-offs of each land use change class. The results of this study can support basin and local land development policy to control sediment losses during development.

Keywords: Chao Phraya River Basin, Distributed hydrological model, Land use change (LUC), Suspended sediment (SS) load

Introduction

Comprehensive sediment management plays an important role in preventing decreases in water-holding ability, mitigating flood damage, controlling reductions in the productivity of farmlands, and maintaining natural river ecosystems [1]. The global population is growing; accordingly, food demand is also increasing rapidly [2]. As a result, it has become essential to develop more farmland to produce more crops; such overuse of resources will eventually lead to soil degradation. Then, the pressure to seek new farming areas could increase further. During the last 40 years, nearly one-third of the world's arable land was lost to erosion, with continuous loss at a rate of more than 10 million hectares year[-1] [3]. Moreover, Southeast Asia has the most serious soil erosion potential at present [4]. At the basin scale, human activities such as deforestation, dam construction, and the use of agricultural chemicals can result in coastal erosion, nutrient enrichment, and dam sedimentation. These problems may become more serious in future owing to climate variability and change and land use development due to rapid population growth.

Different methods have been developed to assess erosion and sediment transport over the past four decades. The universal soil loss equation (USLE) [5] and its revised equivalent (RUSLE) [6] are widely used as empirical soil erosion assessment tools. USLE can simulate long-term (e.g., 20 years) soil erosion for field or farmland units, although it does not consider deposition processes [7]. The European soil erosion model [8] was designed as an event-based model; accordingly, its transport processes do not consider sediment dynamic processes, such as deposition and detachment in river systems, separately. In addition, the water erosion prediction project, a process-based and distributed-parameter computer simulation model, can be applied only to small watersheds [9]. Typically, sedimentary processes in channels and on hillslopes are not simulated separately in existing models [10], and fluvial processes are thought to be more complex for larger catchments. Therefore, a model is required that is applicable for sediment simulation in large river basins and that can consider heterogeneity in processes.

Nowadays, large river basins are undergoing dramatic changes in land use and dam construction due to population growth. Thus, it is becoming critical to develop large basin-scale models that can incorporate climate change, management of the water supply in arid regions, large-scale flooding, and off-site impacts of land management. The soil and water assessment tool, which is a semi-distributed conceptual model, was designed for application in large river basins and for long-term simulations [11]. However, such semi-distributed models do not incorporate higher degrees of spatial information, such as land use and soil type, which are the dominant factors affecting soil erosion. Tang et al. [12] were able to quantify decreases in inflow and deterioration of water quality due to the effects of LUC and climate variability using a geomorphology-based model for non-point source pollution, as reported for the Miyun reservoir in northern China, which covers an area of 15,788 km^2. However, to date, only a few studies have reported sediment modeling for large river basins with drainage areas greater than 100,000 km^2.

The main aim of this study is to assess the effect of land use change on river streams and suspended sediment (SS) load using a process-based distributed modeling approach. The soil erosion process is modeled as the detachment of soil by raindrops and overland flow on hillslopes, considering the transport capacity and deposition processes of a river system. Furthermore, sedimentary processes for the hillslope and channel units are simulated separately in this model.

Study Area

Geographically, Thailand can be divided into four regions: North Thailand; Central Thailand or the Chao Phraya River basin; Northeast Thailand; and South Thailand or the Southern Peninsula. The Chao Phraya River basin covers approximately one-third of Thailand, corresponding to approximately 160,000 km^2.

In this study, the target basin is the gray highlighted area in Figure 1, from the head of the river to the Chao Phraya Dam (C13), covering an area of 117,375 km^2. The basin is traditionally the center of rice production because the monsoon weather typically brings increased rainfall from May to October. Annual precipitation in the Chao Phraya basin varies within the range 1,000–1,500 mm. In addition, the annual average evaporation rate is 1538 mm yr^{-1} and the annual average height of runoff is 200–300 mm. The Chao Phraya River has four major tributaries: the Ping River (36,018 km^2), Wang River (11,708 km^2), Yom River (24,720 km^2), and Nan River (34,557 km^2). Two major dams, the Sirikit and Bhumibol dams, have been in operation since 1972 and 1965, respectively. The operation of these dams helps reduce flooding further downstream, where large cities such as Bangkok and Ayutthaya are located [13]. However, dam construction decreased both bed

and suspended load concentrations in the downstream region and may have affected geological formations through processes such as coastline retreat and land subsidence.
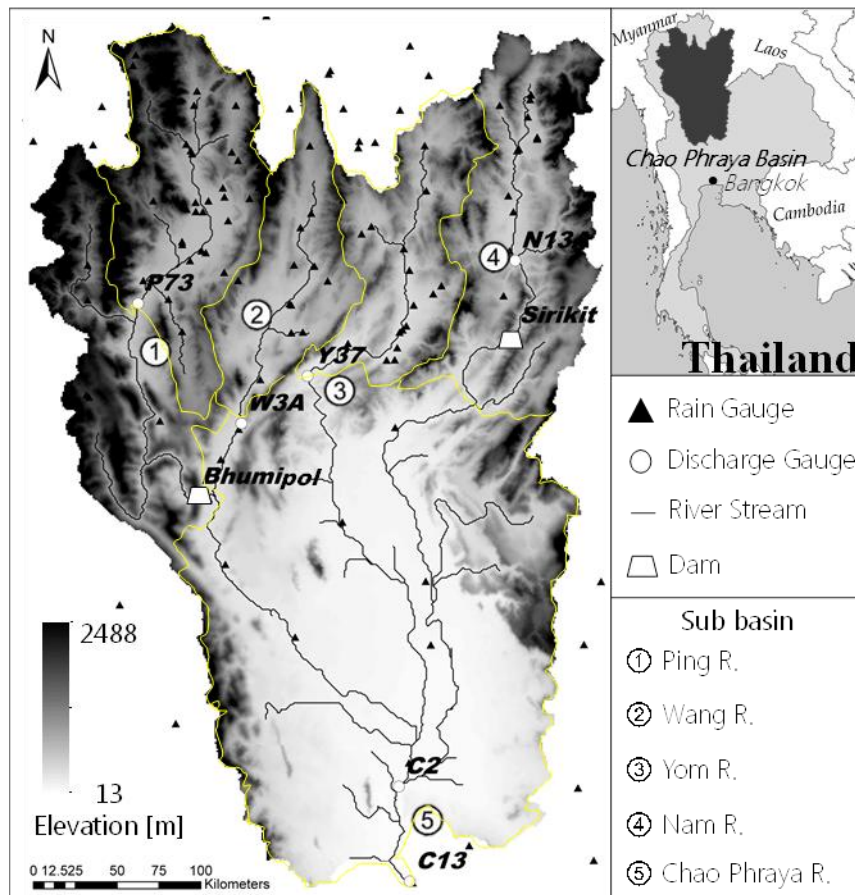

Figure 1. Map of Kingdom of Thailand and the Chao Phraya River Basin and 4 major sub basins

Methodology

Data Sets

Daily precipitation data were collected from two different rain gauge networks. The first is an open-source rain gauge network, with data provided by the Royal Irrigation Department (RID) of the Hydrology and Water Management Center for the Upper Northern Region. The other is managed by the Thai Meteorological Department (TMD). Both datasets offer daily temporal resolution. The locations of the rain gauges are shown as triangles in Figure 1. Geographical information (e.g., topography, soil type, land use) was collected for use in a hydrological model. A digital elevation model (DEM) was obtained from Shuttle Radar Topography Mission data (URL:http://dds.cr.usgs.gov/srtm/version2_1/SRTM3/), which have a spatial resolution of 90 m. For soil type classification, the Digital Soil Map of the World version 3.6 from the Food and Agriculture Organization of the United Nations was used. The dominant soils included sandy clay in the upper region and sandy silt in the lower region. Daily evaporation data were collected from the TMD. Land use pattern datasets were obtained from the Land Development Department of Thailand. The 2001 data (LU_1) are at a scale of 1:50,000, whereas the 2010 data (LU_2) are at a scale of 1:25,000. The land use categories adopted are paddy field, farmland, forest, grassland, bare

land, urban area, and water body. Forest and paddy field are dominant in the northern area and the downstream region, respectively. Observed river discharge and sediment load data were obtained at four discharge gauges in the upper region (P73, W3A, Y37, N13A) and one discharge gauge at the outlet (C2) (Figure 1); these data were used for calibration and validation of the model.

Hydrological Modelling

The distributed hydrological model employed in this study is a geomorphology-based hydrological model (GBHM) developed at the University of Tokyo [14]. It solves the continuity, momentum, and energy equations using two modules: a hillslope model module and a river routing module (Figure 2).
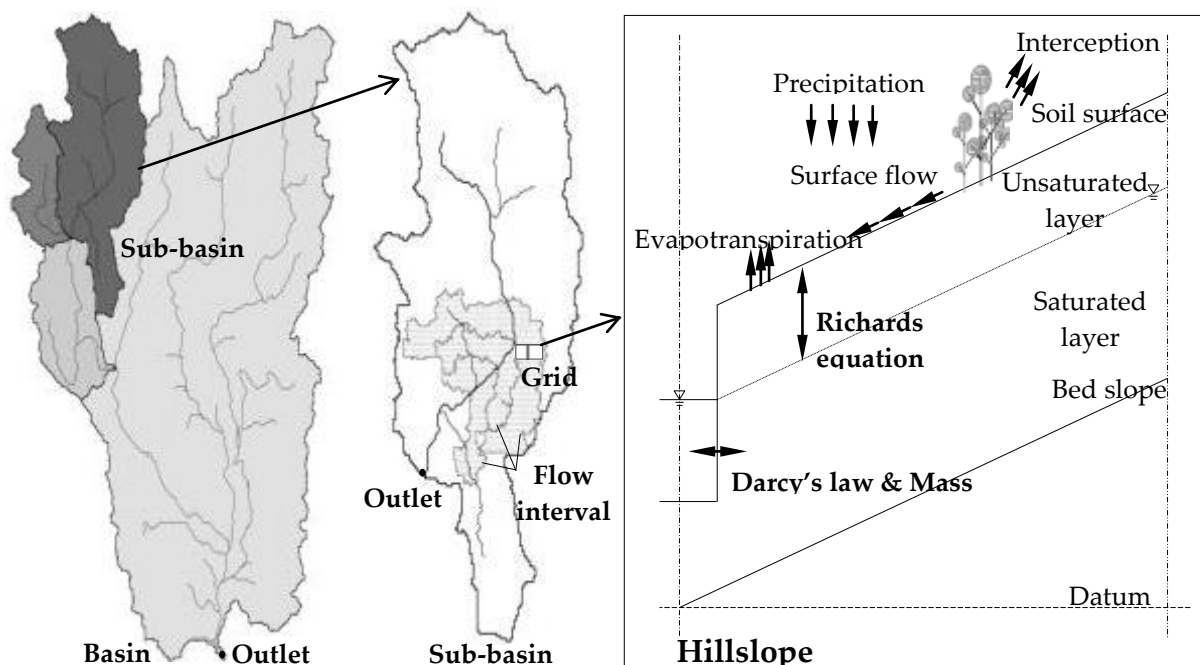

Figure 2. The concept of hillslope based DHM where hydrological processes and river routine take place

In the calculation process, the target watersheds are divided into grids to produce a river network based on flow direction and accumulation in the DEM. The DEM is divided into sub-basins whose outlets occur at the confluences of rivers. In each sub-basin, flow intervals are determined as a function of distance from the outlet. Furthermore, lateral flow to the main stream is estimated by accumulating the runoff at each grid square into one hillslope unit. This is a simplification and means that all hillslopes for a given flow interval drain into the main stream. The flow interval-hillslope system enables GBHM to attempt a fast computation event for a large basin using a physically-based model with the ability to represent spatial variability. The hillslope unit is viewed as a rectangular inclined plane with a defined length and unit width. The inclination angle is given by the surface slope. In the hillslope module, the vertical plane is divided into several layers, including the canopy, soil surface, unsaturated zone, and groundwater. This module calculates hydrological processes such as canopy interception, evapotranspiration, infiltration, and surface flow, as well as exchanges between groundwater and surface water.

The canopy and lower vegetation cover the surface soil, interrupting the direct effects

of raindrops on the soil. The effects of canopy interception on reducing raindrop effects are calculated based on vegetation coverage and leaf area index. The evapotranspiration module simulates the water volume evaporated from surface soil and transpiration from the canopy, although pan observations can also be used. In the module, the Priestley–Taylor method is applied to canopy water storage, the root zone, surface storage, and the soil surface. To describe unsaturated zone water flow, a vertical one-dimensional Richard's equation is used with soil infiltration rate and soil moisture content in the root zone. Saturated water flow and exchange with river water are described using basic equations, including mass balance equations and Darcy's law. Simulation using the surface flow module estimates the infiltration and saturation, discharging excess water into the river system as lateral flow.

In the river routing system, the Pfafstetter numbering method is applied to track water flow efficiently from upstream to downstream. The water routing of the river network is determined along the river stream using one-dimensional kinematic wave equations. This allows us to compute discharge at each gauge point, even in large catchments. However, dams and reservoirs within the river stream disconnect the system. Therefore, the simulated river discharge into the dam is replaced by the observed outflow from the dam using the dam module. The balance of dam inflow and outflow is described according to changes in storage with time according to equation (1). Basically, reservoir routing uses mathematical relationships to calculate outflow from a reservoir once inflow, initial conditions, reservoir characteristics, and operational rules are known [15]. For the simulation in this study, the observed data were used as the dam outflow to obtain the correct river discharge in the lower region. Here, I_{sim} is inflow, O_{obs} is outflow, and dS is change in storage volume.

$$I_{sim} - O_{obs} = \frac{dS}{dt} \tag{1}$$

This hydrological model is effective for the risk assessment of flooding at the basin scale owing to its ability to consider the spatial heterogeneity of data. The model has been applied successfully in studies investigating flood event simulation in the upper Tone River in Japan [16] and for hydrological trend analysis in the Yellow and Yangtze rivers in China [17]. Furthermore, the possibility of combining the model with an atmospheric model to consider dam effects has been demonstrated previously in the Chao Phraya basin [18]. Further details regarding the equation involved in the development of GBHM were provided by Yang et al. [18].

Process Based Soil Erosion and Sediment Transport Module

This modeling approach includes sediment dynamic processes (soil erosion, sediment transport, deposition) integrated into a process-based distributed hydrological model. In the sediment module, sediment dynamics on hillslopes and in river channels were modeled separately and linked to each other systematically.

Hillslope Erosion Process

Hillslope erosion is divided into two systems: detachment due to raindrops and overland flow. In equation (2), soil erosion due to raindrops is calculated based on the canopy ratio, rain intensity, and surface water depth using the following equation [19]:

$$D_R = (1 - C_g)k_r(KE)e^{-zh} \tag{2}$$

where D_R is soil detachment due to raindrop impact (g m^{-2} s^{-1}) and k_r is an index of the detachability of the soil (g J^{-1}), which is set to 5.0 here. KE is the total kinetic energy of

the rain ($J\ m^{-2}$), z is an exponent in the range 0.9–3.1 (set to 3.0 here), h is the depth of the surface water layer (mm), and C_g is the proportion of canopy cover in each grid.

In equations (3, 4), soil erosion by sheet flow on the surface occurs when the hydraulic shear stress exceeds the critical hydraulic shear stress, according to the following equation [20]:

$$D_F = K_f \left(\frac{\tau}{\tau_c} - 1 \right) \quad (\tau > \tau_c)$$ (3)

$$D_F = 0 \qquad\qquad (\tau < \tau_c)$$ (4)

where D_F is overland flow detachment ($Kg\ m^{-2}\ s^{-1}$) and K_f is an overland flow detachability coefficient ($Kg\ m^{-2}\ s^{-1}$), set to 10 mg m^2 here. Additionally, τ_c is the critical shear stress required for initiation of motion and can be obtained from the Shields curve ($N\ m^{-2}$), and τ is the hydraulic shear stress ($N\ m^{-2}$).

Sediment Transport Process

The eroded soil on each hillslope should flow into the main stream and become dissolved in the suspended load. In equation (5) [21], the process of deposition to the bed or detachment from the bed in river is calculated based on the transport capacity concentration and SS concentration. If transport capacity is larger than Cs, i.e., the sediment concentration in each flow interval ($kg\ m^{-3}$), entrainment occurs. If transport capacity is smaller than Cs, deposition occurs. However, we ignored bed load in this case.

$$DF_{river} = \beta_s w\ v_s\ (TC - C_S)$$ (5)

$$\beta_s = 0.79 e^{-0.85J}$$ (6)

where DF_{river} is the flow detachment or deposition ($m^3\ s^{-1}\ m^{-1}$), TC is the transport capacity concentration ($m^3\ m^{-3}$), w is the width of the flow (m), v_s is the particle settling velocity ($m\ s^{-1}$), β_s is a correction factor to calculate cohesive soil erosion, and J is soil cohesion (kPa).

Reservoir Sedimentation

For reservoir sedimentation processes, the sediment loads deposited in the two reservoirs were calculated according to the Brune curve [22]. The Brune curve is well known as a tool for estimating the capture rate of sedimentation in reservoirs and describes the trap efficiency (ET, i.e., the ratio of sedimentation volume in the reservoir to sediment inflow) based on the reservoir capacity (m^3) and annual inflow (m^3).

The Bhumibol dam is the second largest dam in Thailand and is a concrete arch dam with a height of 154 m, crest length of 486 m, total retention volume of 13,462 M m^3 (C), and annual inflow of 6037 M m^3 (I_B). The sedimentation volume is estimated to be 3,800 M m^3. Thus, the effective storage capacity is 9,662 M m^3. The Sirikit dam, which is the third largest dam in Thailand, is an earth fill dam. It has a height of 113.6 m, crest length of 810 m, total retention volume of 9,510 M m^3 (C), and annual inflow of 6452 M m^3 (I_S). The sedimentation volume is estimated to be 2,850 M m^3. Thus, the effective storage capacity is 6,660 M m^3.

In this case, the C/I_B and C/I_S ratios are 2.23 and 1.49 for the Bhumibol and Sirikit dams, respectively. According to the Brune curve, ET is close to 95% for these dams. Thus, in this study, we assumed that 95% of the suspended sediment load was deposited in these two reservoirs.

Model Calibration and Validation

The simulation was run for 10 years spanning 2001–2010 and five stream gauges were used for calibration and validation. Taking into account the availability of data, the daily discharge and sediment data for the year 2001 were used for calibration. Meanwhile, the 2002–2010 data were used for validation. For calibration of parameters related to hydrological and soil erosion process, a semi-automatic calibration method was implemented using a shuffled complex evolution algorithm [23] to identify suitable parameters based on a preliminary sensitivity analysis for the 2001 data. The saturated hydraulic conductivity of the surface soil (ksat1), the hydraulic conductivity of groundwater (kg), and the residual soil moisture (wrsd) were the hydrological parameters calibrated. The calibrated parameters for the sediment transport model were soil detachability by raindrops (kr), detachability due to sheet flow (Kf), and soil cohesion (J).

Results and Discussion

Simulation of River Discharge

River discharge was simulated and the results were combined with dam operation information for 2001–2010 based on two river stream gauges, in the upper region and at the outlet (C2), as shown in Figure 3.

The model was validated at all available river stream gauges with two efficiency criteria: the Nash–Sutcliffe efficiency (Nash) and the correlation coefficient (R). These criteria helped demonstrate the model's applicability, as shown in Table 1. The values of Nash and R were closest to 1 for the Ping River, compared with the other drainage basins. Nash was lowest at gauge C2, which is located in the downstream region, possibly owing to the gently sloping topography in this area, which encourages overflow in the mid-stream section of the Chao Phraya River. Normally, river discharge overflow causes inundation every year during the rainy season in the downstream region because the discharge capacity around C2 is low. Therefore, overestimated discharge naturally overflows to land in real situations. In addition, surface water can inflow smoothly to the river channel in the upper mountainous region; then, its discharge flows down at a steep slope (3.1%). Conversely, the average stream gradient is 0.008% in the lower part of the basin. Such conditions increase the retardation time and reduce river discharge in the lower part of the basin; the resulting floods in this basin can occur over a month, as they did in 2011 [24]. In addition, water withdrawal for irrigation canals can compound these effects.

Table 1. Performance Indicators from Monthly River Discharge

BasiBasin Gauge name	Ping P73	Wang W3A	Yom Y37	Nan N13A	Chao Phraya C2
NSE	0.89	0.91	0.82	0.83	0.69
R	0.95	0.90	0.94	0.94	0.94

Simulation of Suspended Sediment Load

Comparison between simulated and observed SS loads was conducted during the analysis years with available observation data (2001–2010), as shown in Figure 4. Nash and R were used to validate the model's performance. The results in Figure 4 capture the trend in SS load. As shown in Table 2, the values of Nash and R from the stream gauges in the upper sub-basins were greater than 0.5, whereas those from the downstream area (i.e., C2) were underestimated and lower. Fundamentally, the simulation error was greater in the downstream reaches because this uncertainty tends to be accumulated. Additionally, the SS

load was calculated based on its concentration and river discharge, such that the performance of the SS load simulation itself must be related to that of the river discharge simulation.
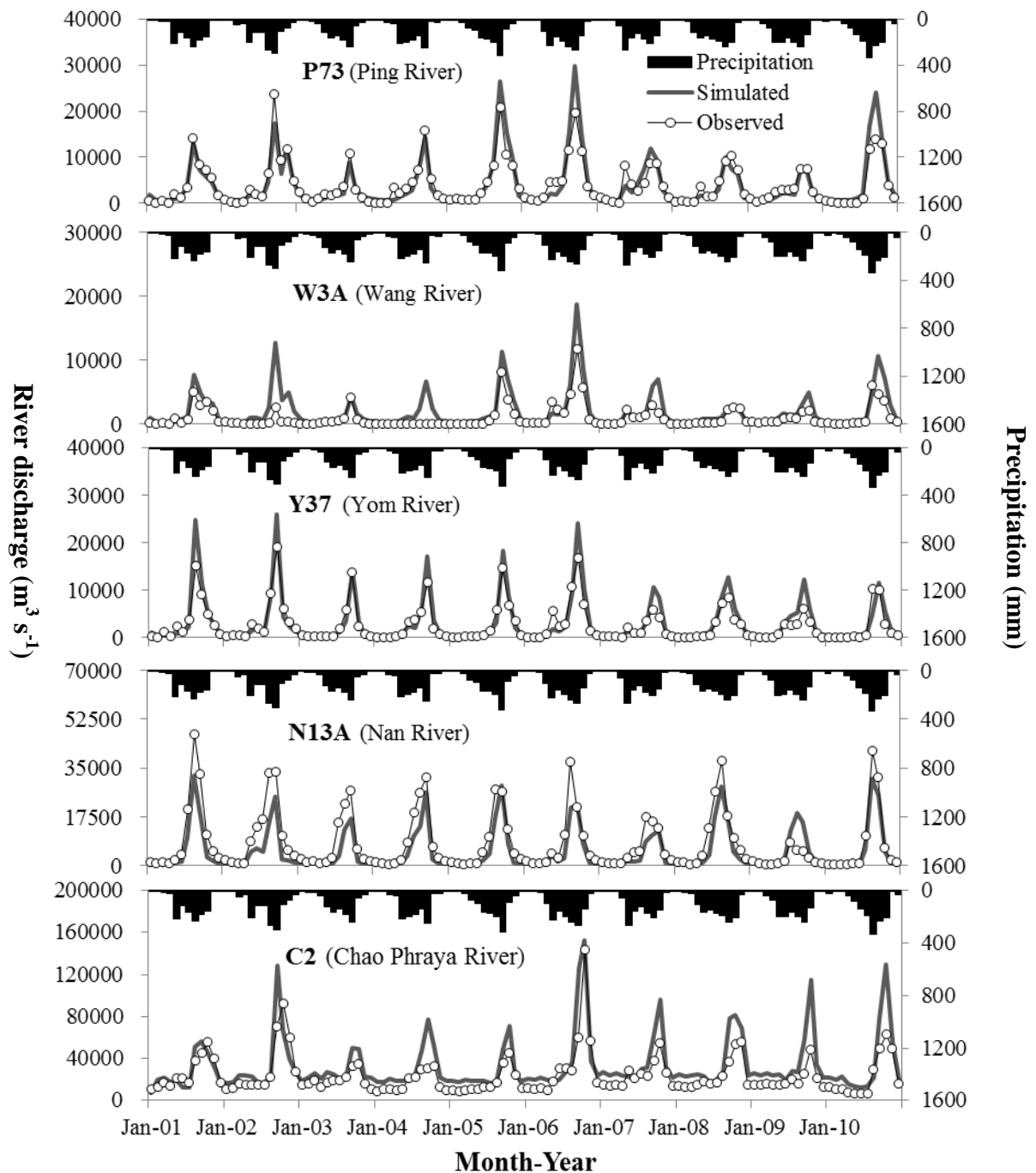

Figure 3. Monthly simulation of river discharge ($m^3 s^{-1}$) at Ping, Wang, Yom, Nan and Chao Phraya River Basin for 2001-2010

There are several possible reasons for the underestimation of the SS simulation in the Chao Phraya River basin. First, the reliability of the observation data may be compromised because RID uses a depth-integrating sediment sampler to measure the daily load, which is subject to human error. Second, the presence of point sediment sources may affect the results. Our model can consider non-point sources of soil erosion, such as overland flow

erosion or river bank erosion. However, in general, landslides occur frequently in mountainous regions and can have a considerable effect on SS concentrations over short periods. Additionally, sand mining sites may be present in the middle reaches and sediment harvesting along the channel could affect the downstream area.
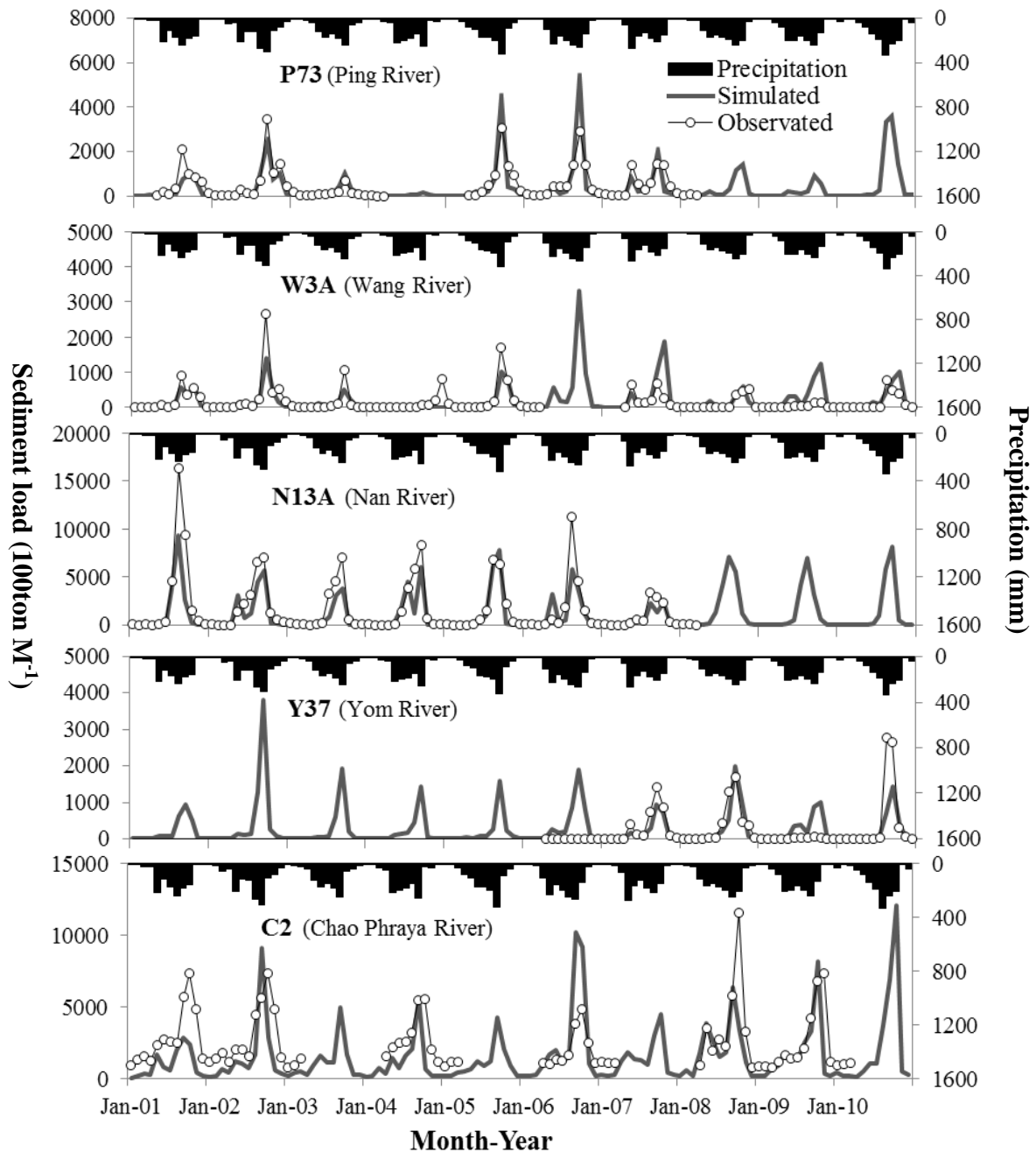

Figure 4. Monthly simulation of sediment load (100 ton month^{-1}) at Ping, Wang, Yom, Nan and Chao Phraya River Basin for 2001-2010

Table 2. Performance Indicators for Monthly SS Load

Basin	Ping	Wang	Yom	Nan	Chao Phraya
Gauge name	P73	W3A	Y37	N13A	C2
NSE	0.55	0.78	0.51	0.72	-0.15
R	0.84	0.67	0.71	0.89	0.56

Simulation of Suspended Sediment Yield

The spatially averaged distribution of annual SS yield was simulated using LU_1 (right panel in Figure 5) in 2001–2010 as input data. The simulated SS yield is shown in the left panel of Figure 5. The mean value is 107.0 (ton year^{-1}km^{-2}) and the total value for the entire basin is 12.6 (M tons year^{-1}). When considering land use pattern, sediment can be yielded by both paddy fields and farmland. Conversely, soil erosion is less pronounced in forest areas, even in mountainous regions. The average eroded soil weights from paddy fields, farmland, and forest were 166.9, 112.8, and 80.1 (ton year^{-1} km^{-2}), respectively. This trend can be attributed to the degree of land cover, with more severe erosion occurring in areas with more sparse vegetation cover. The range of SS yield in the Chao Phraya River basin was compared with that found in previous studies. Three analysis scales were used to obtain SS yield, as shown in Figure 6: the sub-basin, flow interval, and grid scales. In the calculation, the Chao Phraya basin was divided into 25 sub-basins according to the Pfafstetter numbering method. In each sub-basin, flow intervals were determined as a function of distance from the outlet. As the analysis scale increased, the SS yield approached 107 (ton year^{-1}km^{-2}), which is the mean value for the entire basin. This average value can be considered acceptable based on comparison with previous studies conducted by Walling and Webb [25] and Habib et al. [26].

Walling and Webb [25] analyzed sediment load data from 2,000 rivers worldwide and derived a global soil denudation map following Fournier's work in 1987. Based on the results, they reported a SS yield of 50–250 (ton year^{-1} km^{-2}). Conversely, Habib et al. [26] selected 14 sub-basins in the Chao Phraya basin and analyzed sediment yields in 1997 based on observed sediment runoff data, obtaining SS yields of 11–166 (ton year^{-1} km^{-2}). These previous studies investigating SS yield were conducted only at the drainage basin scale or sub-basin scale. Conversely, the present study was able to produce results at a 1-km-grid scale, which is the GBHM computation unit. This possibility of identifying relevant soil loss areas at finer resolution is the primary advantage of this grid-based model. In the upper mountainous region, soil production is concentrated near the river channel. Conversely, in the downstream region, soil loss can occur even far from river stream. Additionally, soil loss at finer resolution tends to be more localized, which is helpful for proper land development practices.

Sediment Budget Concept

The sediment budget concept was applied to ten years of data, as shown in Figure 7. Soil loss from hillslopes is typically transported as runoff, variously ending up in deltas, river deposits, dam deposits, and suspended matter. Here, the two major dams in the study area are the Bhumibol and Sirikit dams. Sediment yield from hillslopes also involves the sediment volume that can potentially be eroded but may not be transported to the channel, instead remaining on the hillslope; this must be accounted in the calculations. In Figure 5, the distribution of potential sediment yield is shown, but the eroded soil within grid areas located far from a channel were not considered in our calculations. The volume of river deposition was 4.3 M ton year^{-1}, constituting 34% of the potential eroded soil. Furthermore, deposition was the dominant process in the Chao Phraya River basin owing to the lack of steep mountains and the dominance of gently sloping areas.
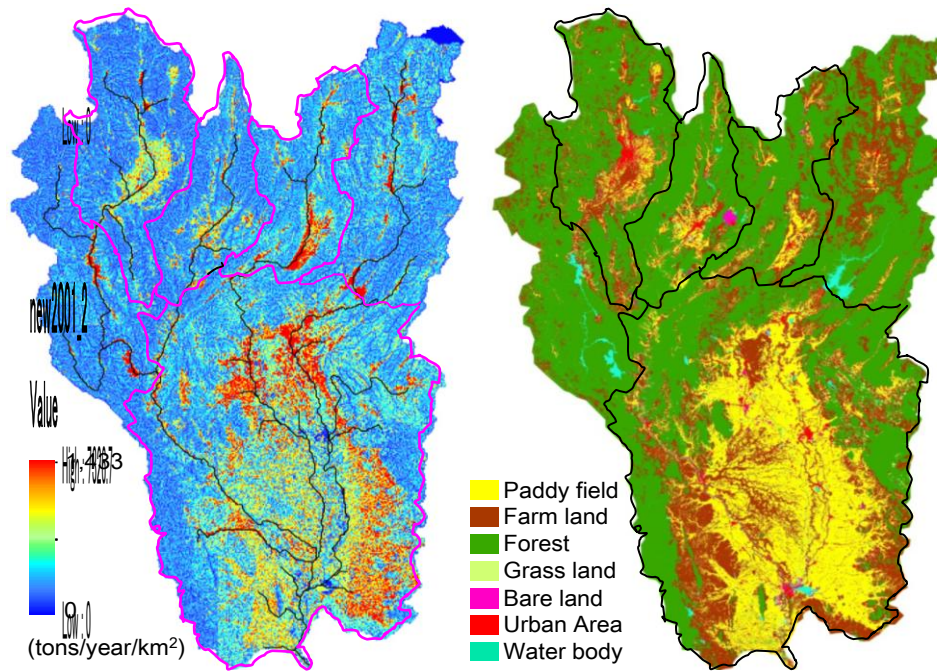
Figure 5. Comparison between simulated annual sediment yields in 2001-2010 (Left panel) and land use map in 2001 (Right panel)
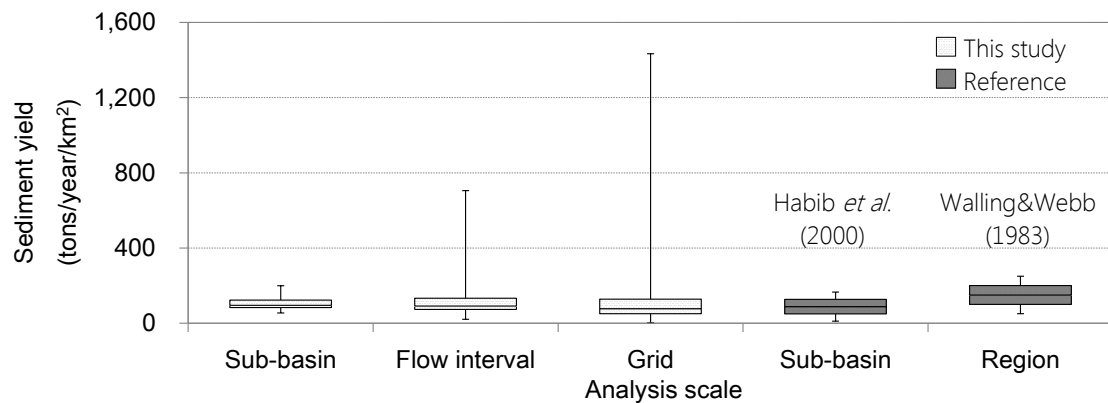

Figure 6. Comparison of the range of simulated sediment yield in 2001-2010 with the results of previous researches by box plot

The volumes of dam deposition and runoff at the outlet were 2.4 M ton year^{-1} (19%) and 1.9 M ton year^{-1} (15%), respectively, whereas the hillslope sediment yield was 3.7 M ton year^{-1} (30%). Sediment yield typically increases in large basins with long hillslope lengths. Accordingly, this concept is important as a sensitivity indicator for the sediment response of catchments. For example, the results demonstrate that only 1/7 of the soil loss in the upper region will eventually be discharged as sediment at C13 in the lower reaches. Thus, the overall sediment delivery ratio was estimated to be only 15% in the Chao Phraya River basin. To define the sediment delivery ratio, the sediment yield at an outlet should be compared with gross erosion within the catchment. Walling and Collins [27] summarized the application of this concept for several basins and found a wide range of delivery ratios (0%–89%), although their study areas were small and medium river basins. This suggests that the implementation of a mitigation strategy to control soil erosion and sediment transport within catchments would not necessarily result in a major reduction in sediment runoff at the outlet of the Chao Phraya basin.
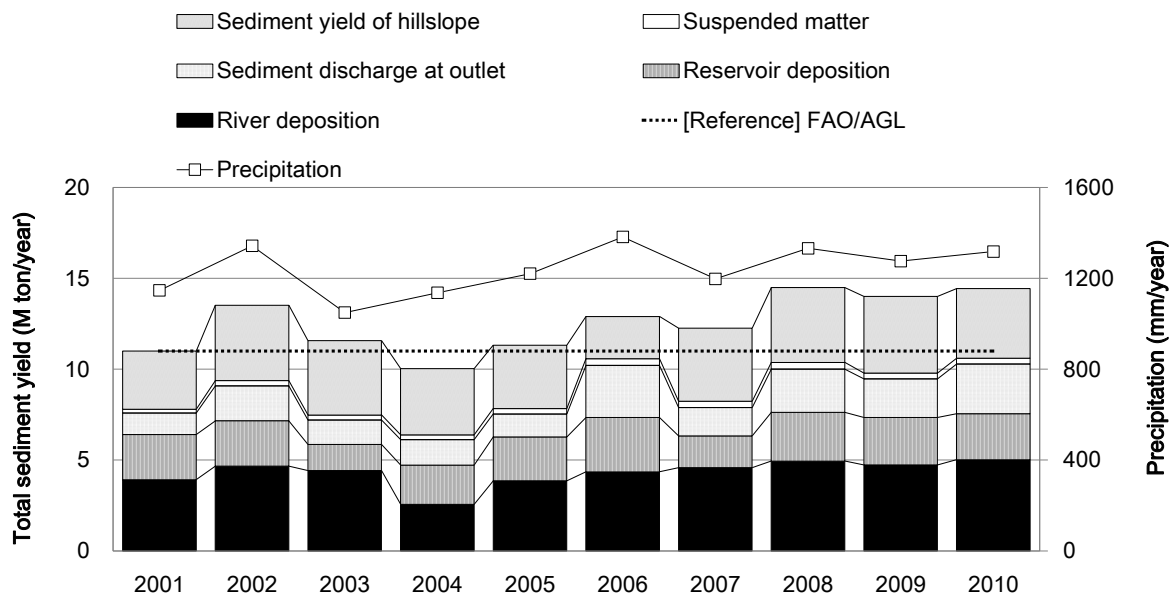
Figure 7. Inter-annual variations in destination composition of sediment yields in 2001-2010 at Chao Phraya Basin

Model Application

Land Use Change Analysis

In this section, a comparison was conducted between the land use patterns in 2001 (LU_1) and 2010 (LU_2). First, overall trends for the whole basin were analyzed (Table 3). The areas of paddy field and forest were found to have decreased over the ten-year period, perhaps owing to the diversion of forest to farmland. Owing to accelerated industrialization in the 1980s, paddy fields bought up by local farmers have been used as farmland for plants before being developed into industrial estates and building sites. Furthermore, reductions in paddy field area have been reported previously for the central region, which is our target area [13]. In the lower region, diversion from paddy field to bare land extended from Nakhon Sawan to Uttaradit. Wang et al. [28] noted that even relatively minor LUC had a significant effect on regional soil erosion rates and sediment transport in rivers and showed that the transformation of forest to farmland exerted the greatest influence. Additionally, the areas covered by other land use types also increased. In particular, the expansion of urban areas was apparent in the upper region, especially around Chiang Mai. Second, the trends for each sub-basin were checked because it was important to quantify the effects within each sub-catchment to help evaluate future conditions considering the social background at the basin level. Clear differences in land use change were found between the Ping, Wang, Yom, and Nan basins (Table 3). In the Ping, Wang, and Yom rivers, the area of farmland increased; conversely, in the Nan River, the area of urban land increased. The most extensive changes occurred in the Ping River basin, although the greatest fractional change occurred in the Yom River.

Table 3. Rate/Area Variation with Land Use Change between 2001 and 2010 in the Chao Phraya River Basin and its Sub Basins

| Land use type | Chao Phraya Basin | | | | Sub Basin | | | | | | | |
| | Area (km²) | | Change | | Ping | | Wang | | Yom | | Nan | |
	In 2000	In 2010	In km²	In %	In km²	In %	In km²	In %	In km²	In %	In km²	In %

Paddy field	24,263	21,390	-2873	-2.4	-430	-2.9	9	0.1	-8	-0.1	-16	-0.2
Farm land	22,071	24,218	2147	1.8	922	6.1	152	1.7	659	6.4	-28	-0.4
Forest	64,554	62,688	-1866	-1.6	-828	-5.5	-11	-0.1	-878	-8.6	28	0.4
Grass land	1,578	2,119	541	0.5	33	0.2	-341	-3.9	69	0.7	-5	-0.1
Bare land	346	620	274	0.2	40	0.3	30	0.3	46	0.4	1	0.0
Urban area	3,434	4,451	1017	0.9	219	1.5	105	1.2	78	0.8	37	0.5
Water body	1,129	1,889	760	0.6	44	0.3	56	0.6	34	0.3	-17	-0.2

Table 4. Effect of Land Use Change on Stream Flow and Suspended Sediment Load from 2001 to 2010 at Ping, Nan, Wang, Yom and Chao Phraya River Basin

		Chao Phraya River		Ping River		Nan River		Wang River		Yom River	
		Change		Change		Change		Change		Change	
		In km^2	In %	In km^2	In %	In km^2	In %	In km^2	In %	In km^2	In %
Streamflow	LU$_1$	394.9		48.5		60.8		23.9		38.6	
(10^3 m^3/s)	LU$_2$	396.8	+0.5	51.5	+5.7	61.0	+0.4	25.6	+6.7	40.4	+4.5
SS load	LU$_1$	187.3		44.9		144.1		24.5		32.2	
(10^4 ton)	LU$_2$	190.4	+1.6	48.3	+7.0	143.3	-0.6	27.7	+11.6	35.0	+8.2

Effect of Land Use Change on River Discharge and Suspended Sediment Load

Table 4 shows the yearly average SS load obtained by simulation under different scenarios, both with and without LUC. The simulation was implemented for all branches. It was estimated that the stream flow and SS load with LU$_2$ had increased compared with the simulation results for LU$_1$ at the gauges in the Ping, Wang, and Yom rivers. Conversely, a reduction in sediment runoff was found at N13A in the Nan River. The change at C2 was also small because the changes in the upper region could be mitigated to some extent by deposition processes and dam effects. From the analysis of LUC described above, we infer that the change in SS load shown in Table 4 was related to the increase/decrease in farmland area. The increasing stream flow can be attributed to loss of forest, which has high surface storage capacity. In this simulation, the surface storage value was 40 mm for forest and 20 mm for farm land. Increases in sediment runoff can be attributed to two reasons. First, forest has a higher proportion of canopy cover in each grid than agricultural land; thus, erosion by raindrops is lower in forest areas. Second, vegetation parameters, particularly Manning's surface roughness, can have a considerable impact on soil loss. Larger roughness values reduce runoff by overland flow because roughness causes considerable friction between sediment particles and the ground surface. In this simulation, Manning's surface roughness was set to 0.15 for forest and 0.04 for farm land. Moreover, the change rates of SS load have always exceeded those of stream flow. Thus, sediment runoff was found to be the factor most sensitive to LUC.

Scenarios Analysis with Deforestation

The analysis in the previous chapter confirms the increasing trend in the Chao Phraya River basin and demonstrates how much the sediment runoff volume increased owing to LUC from 2000 to 2010. However, the effects of farmland alone have not yet been identified. If the extent of sediment runoff decrease in the lower reaches in response to changing land use can be determined, effective countermeasures can be implemented in the

upper region. To achieve a general evaluation, several scenarios with increasing farmland area were applied to the Ping River and Nan River to provide example scenarios. The scenarios developed in this study involve 1% and 5% increases in farmland area by conversion from forest. The random occurrence method in FORTRAN was applied to spatially increase the area. After repeated computation, a new map with a desired percentage increase of farmland was obtained. Ten datasets at each percentage were created randomly. The total volume of SS load over ten years was simulated with both scenarios (i.e., 1% and 5% increase in farmland area) at the P73 and N13A stations, as shown in Figure 8. This figure was obtained after ten times iterations and each plot includes error bars indicating the standard deviation. However, the range was relatively small in the Ping River. Therefore, we infer that the location of the transformation (forest to farmland) did not affect sediment runoff in the Ping River significantly. In fact, the rate of change of sediment runoff appears to be more important than its distribution. The slope and distance from the channel may also act to increase sediment runoff; however, the most dominant factor controlling sediment runoff was in fact the local strong rainfall events scattered spatially throughout the basin. Figure 8 illustrates increasing sediment load with increasing farmland area. These parameters were proportional, with a 0.4% change in sediment load per 1% change in farmland. Conversely, the range of the Nan River was greater than that of the Ping River, which can be attributed to differences in the sediment delivery ratio. Soil erosion can affect the SS load of a basin easily when the basin has a high delivery ratio. The ratio in the Ping River was 39%, whereas that in the Nan River was 105%. Therefore, the Nan River will be most sensitive to the application of a land development strategy to mitigate soil erosion and sediment transport within its catchment. Adoption of the sediment budget concept to determine delivery ratios could provide a useful indicator of the sensitivity of catchments to land development.

Scenarios Analysis with Social Background

Simulations with different scenarios were implemented to evaluate the effect of each land use transformation and manage land use development. Figure 9 shows the results for each scenario. Paddy (−1%) denotes a transformation of 1% of paddy field into farm land, whereas Urban (+1%) indicates a transformation of 1% of forest into urban area. In this case, ten datasets for each scenario were created randomly. The results can be classified into both positive effects (e.g., soil degradation) and negative effects (e.g., soil conservation) for sediment runoff. For Paddy (−1%), the farmland was changed from paddy land because farmers can easily earn a generous salary producing fruit on the converted farmland. This change had a negative effect on sediment load in the lower region, with a ratio −2.0%. For Urban (+1%), forest was changing to urban area in a disordered manner owing to rapid urbanization around Chiang Mai. This change had a negative effect on sediment load in the lower region, with a ratio of −3.0%. The conversion of farmland to forest exerted less pronounced effects on sediment runoff than other conversion types, even though the change in area was greater.
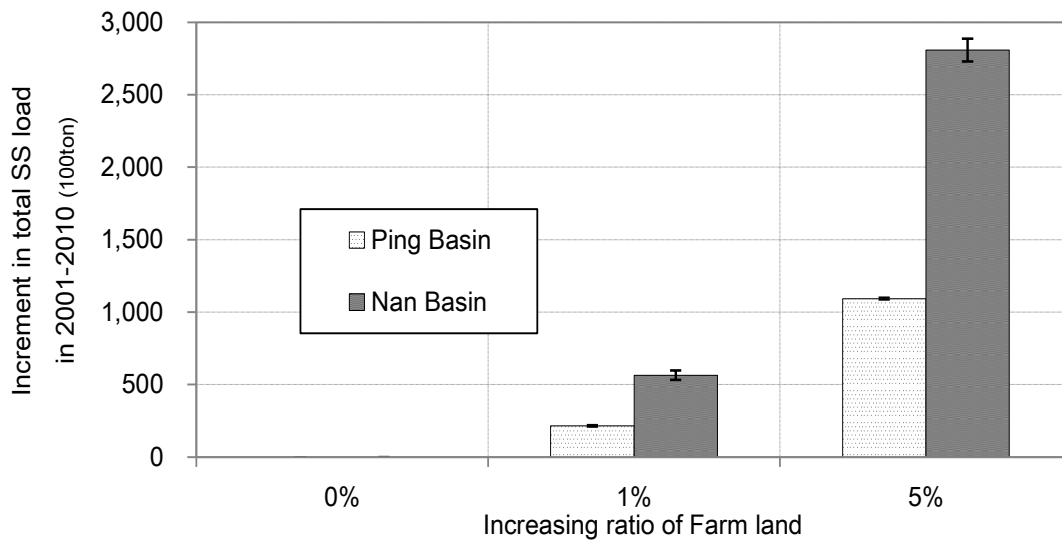
Figure 8. Increment in total suspended sediment load by 1 and 5 % conversion of forest to farm land in 2001-2010 at P73 station in Ping River and N13A station in Wang River
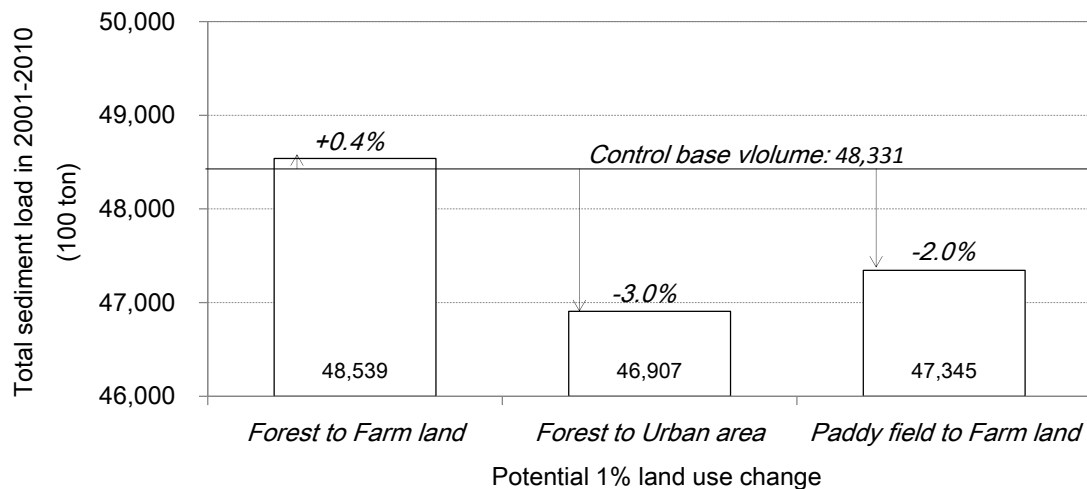

Figure 9. Comparison of total suspended sediment load with 1% potential land use change referring social background in 2001-2010 at P73 station in Ping River

It remains difficult to predict future trends in sediment runoff based on these results. In this analysis, the trend-based method was not applied to the model for future prediction. However, land use development depends on the policies implemented by various departments. For example, as population increases in Thailand, the Ministry of Interior plans to apply a green belt to prevent further disordered expansion of urban areas. However, decreasing the area of available farmland in the near future requires increase in land productivity. In addition, this random expansion of key land use areas could provide information regarding the effects of different types of conversion. Besides the benefits and trade-offs of LUC, the analysis implemented by the model here will be helpful to measure LUC and predict any associated costs. However, these differences type of conversion are meaningful only for the conditions and parameters considered here. For example, when considering future land management, different results may be obtained owing to strong rainfall associated with climate change, as mentioned above. Nevertheless, these results will help support basin management and should be considered in future land management.

Conclusions

In this study, we have demonstrated three steps in the assessment of the effects of land use on river stream and sediment runoff in the Chao Phraya River basin, Thailand: model development, model calibration, and application to Chao Phraya River. A process-based distributed model has been developed for use as part of a comprehensive sediment assessment tool targeting large basins in Southeast Asia.

The simulated results exhibit acceptable agreement with observation data in the upper sub-basins, although the temporal resolution is only at the monthly scale. Conversely, the model simulation results for the lower sub-basin area are underestimated. However, the model performance in the lower sub-basin may be improved further in future research.

The model also successfully simulated the annual average result for different scenario analyses, both with and without land use change. The results indicate reductions in river stream and sediment load in four upper sub-basins of the Chao Phraya River basin. The Wang River basin, covering 11,708 km^2, was found to be the most sensitive sub-basin, exhibiting the highest rate of change. However, the rate of change at the outlet of the simulated area was lower than that in the upper area because the effects in the downstream region can be mitigated to some extent by deposition processes and dam effects. Additionally, this model can be implemented in society as a comprehensive basin management tool. Analysis with various scenarios may be possible for consideration of future land development. Our model can also be applied to other large basins similar to that of the Chao Phraya River.

Acknowledgements

References

[1] J.D. Milliman, Y.A. Qin, M.E. Ren, and Y. Saito, "Man's influence on the erosion and transport of sediment by Asian rivers: The Yellow River (Huanghe) example," *Journal of Geology*, Vol. 95, No. 6, pp. 751-62, 1987.

[2] Food and Agricultural Organization of the United Nations (FAO), *The State of Food Insecurity in the World 2010*, Rome, Italy, 2010.

[3] D. Pimentel, C. Harvey, P. Resosudarmo, K. Sinclair, D. Kurz, M. Mcnair, S. Crist, L. Shpritz, L. Fitton, R. Saffouri, and R. Blair, "Environmental and economic costs of soil erosion and conservation benefits," *Science*, Vol. 267, No. 5201, pp. 1117-23, 1995.

[4] D. Yang, S. Kanae, T. Oki, T. Koike, and K. Musiake, "Global potential soil erosion with reference to land use and climate changes," *Hydrology Processes*, Vol. 17, No. 14, pp. 2913-2928, 2003.

[5] W.H. Wischmeier, and D.D. Smith, *Predicting Rainfall Erosion Soil Losses: A Guide to Conservation Planning*, Agriculture Handbook, No. 282, No. 537, US Department of Agriculture Research Service, pp. 244-252, 1978.

[6] K.G. Renard, and J.R. Freimund, "Using monthly precipitation data to estimate the R factor in the revised USLE," *Journal of Hydrology*, Vol. 157, No.14, pp. 287-306, 1994.

[7] L. Zhang, A. O'Neill, and S. Lacy, "Spatial analysis of soil erosion in catchments: A review of modelling approaches," International Congress on Modelling and Simulation (MODSIM95), *Water Resources Ecology*, Vol. 3, pp. 58-64, 1995.

[8] R.P.C Morgan, J.N. Quinton, R.E. Smith, G. Govers, J.W.A. Poesen, K. Auerswald, G. Chisci, D. Torri, and M.E. Styczen, "The European Soil Erosion Model (EUROSEM): A dynamic approach for predicting sediment transport from fields and small catchments," *Earth Surface Processes and Landform*s, Vol. 23, No. 6, pp. 527-544, 1998.

[9] S. Duna, J.Q. Wua, W.J. Elliot, P.R. Robichaudb, D.C. Flanaganc, J.R. Frankenbergerc, R.E. Brownb, and A.C. Xud, "Adapting the Water Erosion Prediction Project (WEPP) model for forest applications," *Journal of Hydrology*, Vol. 366, No. 1, pp. 46-54, 2009.

[10] M.A. Kabir, D. Dutta, and S. Hironaka, "Process-based distributed modeling approach for analysis of sediment dynamics in a river basin," *Hydrology and Earth System Sciences*, Vol. 15, No. 4, pp. 1307-1321, 2011.

[11] J.G. Arnold, R. Srinivasan, R.S. Muttiah, and J.R. Williams, "Large area hydrologic modeling and assessment part I: Model development 1," *Journal of the American Water Resources Association*, Vol. 34, No.1, pp. 73-89, 1998.

[12] L. Tang, D. Yang, H. Hu, and B. Gao, "Detecting the effect of land-use change on streamflow, sediment and nutrient losses by distributed hydrological simulation," *Journal of Hydrology*, Vol. 409, No. 1, pp. 172-182, 2011.

[13] T. Tebakari, J. Yoshitani, V. Khao-Uppatum, and C. Suvanpimol, "Trend analysis of land use change effect on discharge in the Chao Phraya River Basin," *Journal of Japan Society of Civil Engineers*, Series B1 (Hydraulic Engineering), Vol. 47, pp. 205-210, 2003.

[14] D. Yang, T. Oki, S. Herath, and K. Musiake, "A geomorphology-based hydrological model and its applications," In *Extinction*, V.P. Singh, and D.K. Frevert, eds.: Mathematical Models of Small Watershed Hydrology and Applications, Water Resources Publications, Littleton, Colorado, United States, pp. 259-300, 2002.

[15] V.M. Ponce, *Engineering Hydrology: Principles and Practices*, Vol. 640, Prentice Hall, 1989.

[16] D. Yang, T. Koike, and H. Tanizawa, "Application of a distributed hydrological model and weather radar observations for flood management in the upper Tone River of Japan," *Hydrological Processes*, Vol. 18, No. 16, pp. 3119-3132, 2004.

[17] Z. Cong, D. Yang, B. Gao, H. Yang, and H. Hu, "Hydrological trend analysis in the Yellow River Basin using a distributed hydrological model," *Water Resources Research*, Vol. 45, No. 7, pp. 1-13, 2009.

[18] D. Yang, S. Herath, T. Oki, and K. Musiake, "Application of distributed hydrological model in the Asian monsoon tropic region with a perspective of coupling with atmospheric models," *Journal of the Meteorological Society of Japan*, Vol. 79, No. 1B, pp. 373-385, 2001.

[19] D. Torri, M. Sfalanga, and M. Delsette, "Splash detachment: Runoff depth and soil cohesion," *Catena*, Vol. 14, No. 3, pp. 149-155, 1987.

[20] D.M. Habib–ur–Rehman, and E.M.N. Akhtar, "Development of regional scale soil erosion and sediment transport model; its calibration and validations," In: *Pakistan Engineering Congress*, Vol. 69th Annual Session Proceedings, pp. 231-245, 2006.

[21] R.E. Smith, D.C. Goodrich, and J.N. Quinton, "Dynamic distributed simulation of watershed erosion - the KINEROS 2 and EUROSEM models," *Journal of Soil and Water Conservation*, Vol. 50, No. 5, pp. 517-520, 1995.

[22] G.M. Brune, "Trap efficiency of reservoirs," *Transactions American Geophysical*

Union, Vol. 34, No. 3, pp. 407-418, 1953.

[23] Q. Duan, S. Sorooshian, and V. Gupta, "Effective and efficient global optimization for conceptual rainfall‑Runoff models," *Water Resources Research*, Vol. 28, No. 4, pp. 1015-1031, 1992.

[24] D. Komori, S. Nakamura, M. Kiguchi, A. Nishijima, D. Yamazaki, S. Suzuki, A. Kawasaki, K. Oki, and T. Oki, "Characteristics of the 2011 Chao Phraya River flood in Central Thailand," *Hydrological Research Letters*, Vol. 6, pp. 41-46, 2012.

[25] D.E. Walling, and B.W. Webb, "Erosion and sediment yield: A global overview," *IAHS Publications*, Vol. 236, pp. 3-20, 1996.

[26] D.M. Habib–ur–Rehman, S. Herath, and K. Musiake, "Sediment yield characteristics of Chao Phraya River basin, Thailand," In: *Japan Society of Civil Engineers 55th Annual Session Proceedings*, 2000.

[27] D.E. Walling, and A.L. Collins, "The catchment sediment budget as a management tool," *Environmental Science and Policy*, Vol. 11, No. 2, pp. 136-143, 2008.

[28] G. Wang, J. Xia, and J. Chen, "Quantification of effects of climate variations and human activities on runoff by a monthly water balance model: A case study of the Chaobai River Basin in Northern China," *Water Resources Research*, Vol. 45, No. 7, 2009.